

Surface states, surface magnetization, and electron-spin polarization: Ni(001)

C. S. Wang*

Physics Department and Materials Research Center, Northwestern University, Evanston, Illinois 60201

A. J. Freeman

*Physics Department, Northwestern University, Evanston, Illinois 60201**and Argonne National Laboratory, Argonne, Illinois 60439*

(Received 22 January 1979; revised manuscript received 13 November 1979)

Results are presented of the first *ab initio* self-consistent spin-polarized energy-band study of a ferromagnetic transition-metal film [Ni(001)] that is thick enough (nine layers) to accurately determine the energy dispersion and spatial character of surface states and their effects on the surface spin polarization, surface magnetic moments, and average exchange splittings. Band structures and surface states, layer density of states, and charge and spin densities are presented and used to discuss a number of experiments. We find no evidence for magnetically "dead layers" on Ni(001) surfaces. The surface-layer magnetic spin moment is reduced by 20% from the center-layer magnetic moment (which has the bulk value) due to a majority-spin *d*-hole surface state at \bar{M} which lies just above the Fermi energy.

I. INTRODUCTION

The possible role of magnetic surfaces and interfaces in explaining a number of recently observed phenomena has become a subject of some interest. This renewed interest has been stimulated, in part, by recent developments in experimental methods which have provided unique new information about spin polarization in magnetic materials.¹⁻⁸ Concurrently, advances in theoretical band-structure methods, notably in bulk self-consistent (SC) calculations within the local spin-density-functional formalism (LSDF), have gradually converged on a rather consistent picture of the electronic and magnetic properties of transition metals.^{9,10} In several important cases, however, good agreement between theory and experiment is still lacking.¹¹ For example, whereas earlier electron-spin-polarization (ESP) measurements in spin-polarized photoemission on polycrystalline samples showed positive ESP which was proportional to the magnetization,¹ Eib and Alvarado² found, using single crystals, negative ESP that changed sign abruptly within 0.1 eV of the threshold from Ni(001) and Ni(111). Qualitatively, this result was anticipated by Wohlfarth¹² using a simple model for the bulk density of states (DOS) and by Smith and Traum¹³ using a joint DOS model. Dempsey and Kleinman¹⁴ pointed out that near threshold the conservation of the transverse component of wave vectors upon escape would limit the contribution to regions around $\bar{\Gamma}$ in the two-dimensional Brillouin zone where no propagating bulk states are available on Ni(001); thus, the only allowed transition is an excitation into evanescent time reversed LEED states near the surface. Dempsey and Kleinman found majority-spin $\bar{\Gamma}_5$ sur-

face states (SS) at 0.08 eV below the Fermi energy essential to explain quantitatively the ESP reversal.¹⁵

Electron-spin polarization from a ferromagnetic metal like Ni is only one of a number of fundamental questions about surface magnetism¹⁶; others include the possible modification of the magnetization itself—for which the concept of "dead layers," introduced by Liebermann *et al.*,¹⁷ is the most dramatic. Liebermann *et al.* studied films of Ni, Fe, and Co electroplated onto Cu and Ag substrates and found for Ni a deficiency of magnetic moment when extrapolated to $T=0$ amounting to that expected from two magnetically "dead layers." The theoretical interpretations of this phenomenon has stirred some controversial¹⁸⁻²¹ discussions and some questions about the experimental procedure (including the possible role of impurities at the interface¹⁶). Recently, precise measurements by Bergmann²² showed a large difference in the behavior of the anomalous Hall effect in Ni and Fe films. Apparently, the Ni film becomes ferromagnetic only for films thicker than 2.5 atom layers.

It is clear from the above that theoretical studies of the electronic structure of ferromagnetic metal surfaces are needed in order to answer some of the fundamental questions raised and to provide a framework with which to interpret the experimental observations. Since surface effects depend crucially on the existence, role, and nature of surface states which are highly sensitive to the details of the surface potential, only self-consistent energy-band calculations can be relied upon to properly provide this information. Recently, we presented a self-consistent numerical basis-set linear combination of atomic-orbitals (LCAO) discrete variational method within the

framework of local density-functional theory, for determining the electronic structure of thin films to simulate surface effects on a semi-infinite solid.²³ In its successful application to 1, 3, and 5 layers of paramagnetic Ni(001) films²³ and to oxygen chemisorbed in the $c(2 \times 2)$ configuration,²⁴ the method proved itself to be a powerful theoretical tool for studying surface properties (including chemisorption bonding) of transition metals with their inherent difficulties of describing both the localized d electrons along with the itinerant s - p electrons.

This paper presents the results of our first spin-polarized *ab initio* SC energy-band study of the ferromagnetic Ni(001) surface. It is to be emphasized that the film is thick enough (nine layers) to accurately determine the energy dispersion and spatial character of SS and their effects on the surface spin-polarization, surface magnetization, charge distribution, and layer projected DOS. Among our results, the majority-spin $\bar{\Gamma}_5$ SS is found to be only weakly localized on the surfaces and to contribute little to the surface projected DOS near threshold. We find a majority-spin d -hole SS which reduces the surface spin magnetic moment ($0.44\mu_B$) and exchange splitting (0.41 eV at \bar{M}_3 SS) from their values ($0.58\mu_B$) and 0.63 eV) for bulk ferromagnetic Ni.⁹ No evidence is found for magnetically "dead layers" on Ni(001) surfaces. These results may be important (together with escape depth information) for interpreting recent angle-resolved photoemission experiments.³

II. METHOD

We use our new SC linear combination of atomic-orbitals method for an unsupported thin film,²³ a numerical basis set ($3d$, $4s$, and $4p$) orthogonalized to the (frozen) core wave functions and symmetrized according to the symmetry of the wave vector \bar{k} , and the LSDF exchange and correlation potential of von Barth and Hedin.²⁵ The charge and spin densities are calculated by a linear analytical triangle scheme (described earlier²³) based on a sampling of 15 \bar{k} points in $\frac{1}{8}$ th of the two-dimensional Brillouin zone (BZ). In this scheme the irreducible wedge of the Brillouin zone is divided into 16 triangles, the energies are extrapolated linearly inside each triangle, and the cutoff of the Fermi energy is incorporated exactly within the linear energy approximation. Furthermore, energies of each spin are ordered separately for states of even and odd symmetry with respect to reflection symmetry about the center plane to properly account for anticrossings; if neglected, these could cause significant errors in the linear approximation due to the high density of energy levels. In contrast to the case of charge density, the calculation of the spin density in magnetic metals usually requires higher accuracy in carrying out the required Brill-

ouin-zone integration because it is much smaller. In a very interesting way, the \bar{k} -space integration is related to the layer thickness in the thin-film model. Within the idea of a commensurate cell, an n -layer film is equivalent to sampling the bulk spin density along the surface normal direction of a three-dimensional Brillouin zone using a histogram method with n divisions. This argument provides indirect evidence why the film must be thick enough to describe correctly the spin density at the free surface of a bulk magnetic metal. Hence, in this work we chose a film which is nine layers thick. Such a thick film also minimizes possible interference from SS on opposite surfaces in the film.

Self-consistency is obtained iteratively within the superposition of spherically symmetric atomic charge density model. The final SC potential minimizes the integrated rms difference between the input superposition and output crystal charge densities (0.426 compared to 90 valence electrons in the unit cell). In the last iteration, the layer integrated input and output charge and spin densities agree to within 0.03 electrons and $0.02\mu_B$, respectively. These values may be considered as the maximum limiting uncertainties in the charge and spin densities. Experience with the self-consistent iterative procedure indicates that the actual uncertainties may be considerably smaller. For example, only a small mixing of the new potential ($\sim 10\%$) with the old potential is permitted if the degree of self-consistency is to be improved in the next iteration. Thus, although our final *input* charge density yields a rather consistent result, a potential generated with the corresponding *output* charge density (with an addition of only 0.03 localized $3d$ electrons in the central plane) could easily push more than half an electron into each of the surface layers and cause divergence of the results.

By contrast, the uncertainty in our E_F (Fermi energy) is very large. As we had previously discussed²³ for the paramagnetic Ni(001) films using the Kohn-Sham local density exchange-correlation potential, the least-squares-fitting procedure in our SC process emphasizes the high-density limit (which affects details of the energy bands) more than the low-density region (which tends to shift the potential rigidly). In a SC calculation for a bulk system, the origin of the energy bands has no effect on the electronic wave functions because the solution of Poisson's equation is not affected by a rigid shift in the potential. However, during the course of this investigation, we found that the band structure shifted rigidly without any noticeable changes in the wave functions when the $4s$ and $4p$ atomic configurations are varied in constructing the superposition potential. This is possible because, as demonstrated in Table I, there is a part of the selvage region (near vacuum) where the exchange-correlation potential is large even though the charge density itself is already negligibly small.

TABLE I. Values of the von Barth and Hedin and Wigner exchange-correlation potential versus electron density (in a.u.).

Density (electrons/a.u.)	vBH (eV)	Wigner (eV)
10^3	-272.2	-269.5
10^2	-128.1	-125.9
10	-60.9	-51.2
1	-29.5	-28.2
10^{-1}	-14.6	-13.8
10^{-2}	-7.4	-7.0
10^{-3}	-3.9	-3.7
10^{-4}	-2.1	-1.9
10^{-5}	-1.1	-1.0
10^{-6}	-0.5	-0.5
10^{-7}	-0.3	-0.2
10^{-8}	-0.1	-0.1

(Table I also indicates that *large* differences in the exchange-correlation potentials for different treatments will, as has been found, also affect the calculated E_F .) Since there are hardly any ground-state wave functions to sample the potential in this region, only the origin of the energy band is affected. The wave function remains the same because the solution to the Poisson equation is not changed by a rigid shift in the potential. Thus, uncertainty in the origin of the energy makes it difficult to compare the Fermi energy with the experimental work function; however, the uncertainty in the long tail of the potential has very little effect on the ground-state properties presented in this paper.

III. ENERGY-BAND STRUCTURE

The majority- and minority-spin energy bands along the high-symmetry directions in the BZ are shown in Figs. 1 and 2. In order to clarify the already complex band structure, states of $\bar{\Delta}_2 - \bar{Y}_2 - \bar{\Sigma}_2$ symmetry are displayed above those of $\bar{\Delta}_1 - \bar{Y}_1 - \bar{\Sigma}_1$ symmetry. In addition, the wave functions have either even or odd parity with respect to reflection about the central plane. For a given two-dimensional symmetry, only bands of opposite parity are allowed to cross one another. As in our earlier paramagnetic calculations, the general trends in the energy bands (opening of band gaps, bandwidths, etc.) agree well with the parametrized LCAO calculation of Dempsey and Kleinman¹⁴ for a 35-layer spin-polarized Ni(001) film.

In these figures, the pairs of even- and odd-symmetry SS are denoted either as circles or as triangles pointing toward each other if their degeneracy is

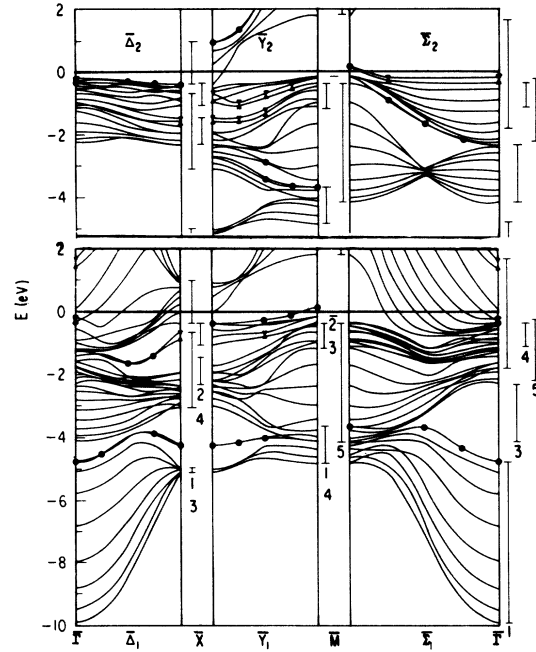


FIG. 1. Majority-spin energy bands of nine-layer Ni(001) film along the high-symmetry directions in the two-dimensional BZ. States of $\bar{\Delta}_2 - \bar{Y}_2 - \bar{\Sigma}_2$ and $\bar{\Delta}_1 - \bar{Y}_1 - \bar{\Sigma}_1$ symmetry are shown in the top and bottom panels, respectively. SS are indicated by circles and triangles.

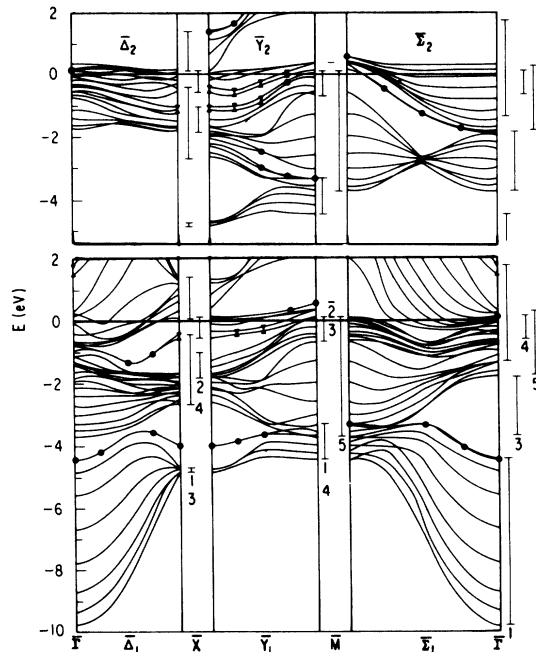


FIG. 2. Minority-spin energy bands of nine-layer Ni(001) film.

split due to the finite thickness of the film. Based on a Mulliken charge analysis, the closed circles and triangles indicate states with more than 75% of their charges localized on the first two surface layers while the open circles and triangles indicate a 50% localization. The $\bar{\Gamma}_{51}$ SS (0.24 eV below E_F) has 29, 27, and 20% while the $\bar{\Gamma}_{41}$ SS (0.33 eV) has 70, 22, and 6% of its density on the first three planes from the surface. Both SS are less localized than those of Dempsey and Kleinman¹⁴ whose $\bar{\Gamma}_{51}$ SS (0.08 eV) has 47, 24, and 13% and whose $\bar{\Gamma}_{41}$ SS (0.18 eV) has 80, 15, and 3.4% of its density on the first three planes. Significantly, our findings of extremely weak surface states near $\bar{\Gamma}$ are consistent with the recent angle resolved photoemission results of Plummer and Eberhardt²⁶ where majority-spin surface states right below E_F are found near the boundary of the BZ but *not* near the zone center.

Let us now consider the very important role played by the SS in surface magnetism. Note that in Fig. 1, the majority-spin $\bar{Y}_1 - \bar{M}_3 - \bar{\Sigma}_2$ levels split away from the bulk continuum right below E_F , become unoccupied and so create a surface majority-spin d hole. By contrast the area of the minority-spin $\bar{Y} - \bar{M} - \bar{\Sigma}_2$ d holes in Fig. 2 is reduced by the lowering of the $\bar{\Sigma}_2$ SS. Both effects tend to reduce the surface magnetic moment from its bulk value and the overall exchange splitting near the top of the d band.

A more dramatic demonstration of this effect is shown in Figs. 3 and 4 where, based on the idea of a commensurate cell,^{23,27} we compare the projected two-dimensional bands (solid curves) at $\bar{\Gamma}$, \bar{M} , and \bar{X} points with the bulk band structure of Wang and Callaway⁹ (solid lines) along the surface normal directions [Δ , Z , and Γ to (π/a) (1,1,0)] with their Fermi energies aligned. Note that in the limit of infinite

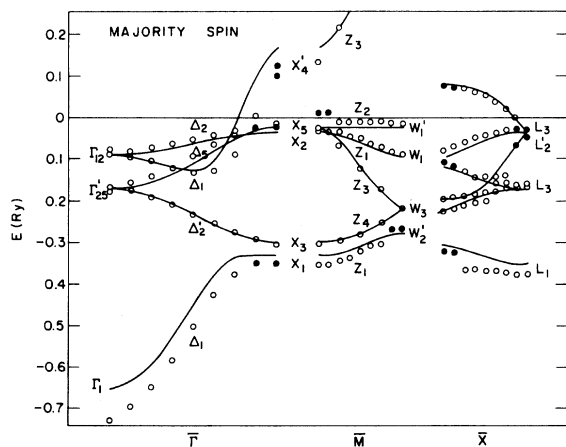


FIG. 3. Comparison of the projected two-dimensional bands and the bulk band structure (solid curves) of Wang and Callaway (Ref. 9) for majority spin. The surface states are indicated by filled circles.

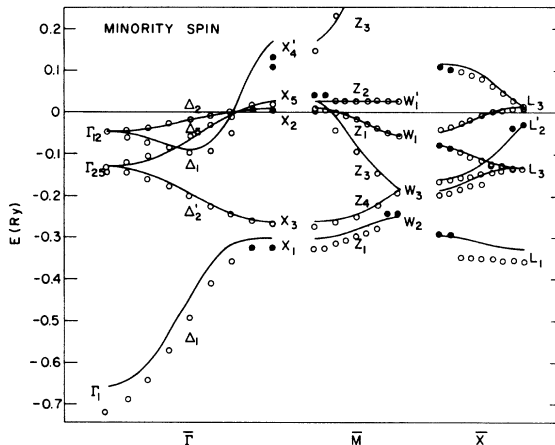


FIG. 4. Comparison of the projected two-dimensional bands and the bulk band structure (solid curves) (Ref. 9) for minority spin. The surface states are indicated by filled circles.

film thickness, the energies at a point \bar{k} in the two-dimensional BZ span all the points at $(\bar{k}, k_z) + \bar{K}$ in the three-dimensional BZ where $-\pi/a \leq k_z \leq \pi/a$. For a finite number of atom planes, n , there are only n energies at a point \bar{k} and hence only n points in plots such as in Figs. 3 and 4. In Figs. 3 and 4, the SS that split away from the bulk are indicated by closed circles. The splitting away of the majority-spin \bar{M}_3 SS from the bulk $W'_1 - Z_2 - X_5$ level which crosses the Fermi energy can be seen clearly in the center panel of Fig. 3. In general, as shown in Figs. 3 and 4, we find very good agreement with the bulk results throughout the d -band complex while the surface sp-states lie slightly lower due to the reduction of the exchange potential near the surface.²³ Note that the nearly degenerate \bar{M}_2 and \bar{M}_3 states (which correspond to the bulk $W'_1 - Z_2 - X_5$ line) are magnetically split by 0.53 eV; this splitting is smaller than the theoretical bulk value⁹ of 0.63 eV. The splitting of the corresponding surface states is 0.41 eV.

IV. DENSITY OF STATES

The local DOS (projected by a Mulliken analysis) are shown in Fig. 5. The center plane DOS agrees very well with the bulk results⁹ (bottom panels) while the surface plane DOS shows a significant narrowing of the d -band width and a shift of peak positions. The upward shift of surface DOS can be foreseen in Figs. 1 and 2 where a large number of SS are found in the region 0 to 2 eV. The sharp structure found by Dempsey and Kleinman¹⁴ in their majority-spin surface DOS right below the Fermi energy (essential to their explanation of the ESP reversal) does not ex-

ist in our result. Recently, Moore and Pendry²⁸ have calculated the ESP on Ni(001) including the band structure (obtained with a non-SC muffin-tin potential with a simple step surface potential barrier), scattering of the outgoing wave, and lifetime effects. Without invoking SS they found good agreement with experiment² when a bulk exchange splitting equal to 0.33 eV was chosen. This close agreement further supports our results for the role of the $\bar{\Gamma}_5$ SS in the interpretation of the experiment.

The d -band width for Ni reported by Eastman *et al.*³ (3.4 eV at L) is also smaller than the theoretical estimate of the bulk values (4.8 eV). Pendry and Hopkins²⁹ have proposed that in the angular-resolved photoemission of Eastman *et al.*,³ the bottom of purely d states are washed out by excessive lifetime broadening of the d holes while the wider d -band

width reported by Smith *et al.*⁸ arises from the longer hole lifetime of $sp-d$ hybridized state. However, neither the surface d -band narrowing nor the lifetime broadening can be used to explain the difference between optical and magneto-optical properties of bulk Ni calculated with matrix elements using wave functions including spin-orbit coupling³⁰ and experiment. A large broad structure beginning around 4 eV is displaced in theory to higher energy by 0.8 to 1 eV.

Although our results show that the exchange splitting and the d -band width is slightly reduced on the surface, the reduction is too small to account for the discrepancy between the theoretical studies for bulk systems and the experimental measurements. The remaining difference between theory and experiment implies either (i) the failure of the LSDF approximation (which almost all first-principles band calculations rely on) to describe the ground-state properties for ferromagnetic Ni, or (ii) there are substantial many-body effects (electron-magnon, electron-hole interactions). The latter is the common factor neglected in the band-theory interpretation of the optical and photoemission (excited-state) experiments.

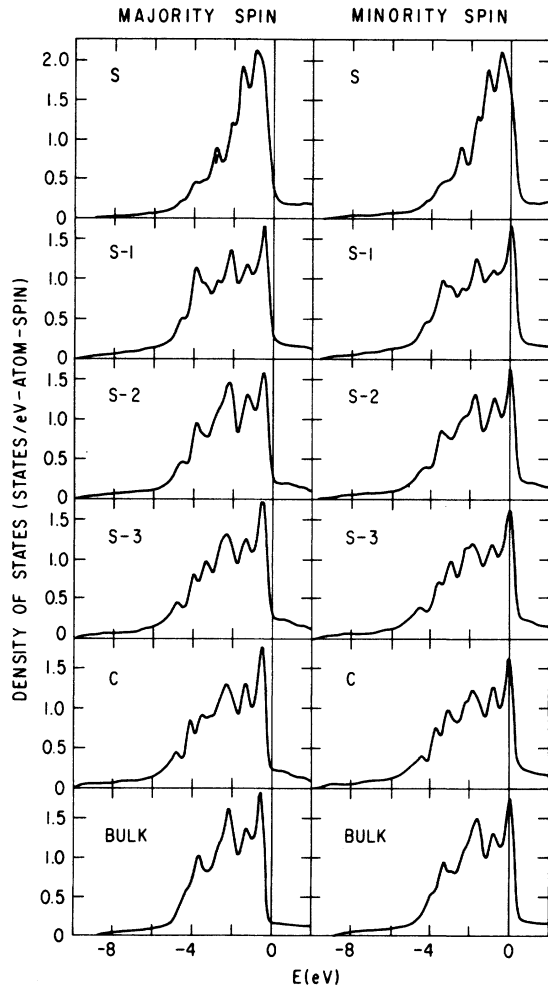


FIG. 5. Layer projected DOS including a Gaussian broadening function of 0.3 eV FWHM. The bulk DOS of Wang and Callaway (Ref. 9) for ferromagnetic Ni is shown in the bottom panel for comparison.

V. SURFACE MAGNETISM

As an indication of the results obtained, we show in Figs. 6 and 7 self-consistent charge- and spin-density maps on the face of the cube (vertical axis along [001]), i.e. on the (110) plane. The charge density is surprisingly bulklike starting at one layer below the surface plane. As one enters the surface region, the charge density gradually becomes smooth and parallel to the surface. Around each atom, there is a fairly large region where the charge density is spherically symmetric in confirmation of the often-made muffin-tin approximation, except in the interstitial region on the surface plane where the charge density varies more rapidly due to the open surface structure. In very good agreement with the bulk results,⁹ the spin density is larger along the [110] than along the [001] direction. In the interstitial region (where the sp electrons dominate), the spin density, shown as dashed lines, is negative. This opposite polarization of the sp to the d electrons in a large surface region, as well as in the bulk, may be important in interpreting spin-polarized tunneling,⁶ field emission,⁵ and electron capture⁷ experiments because the matrix elements for the extended sp electrons may be considerably larger than those for the localized d electrons.

From the self-consistent total charge and spin densities we may determine layer-plane distributions. Using a nearest volume integration, our results yield a practically neutral charge density around each atom (10.02, 9.97, 9.97, 10.02, and 10.05 electrons on sur-

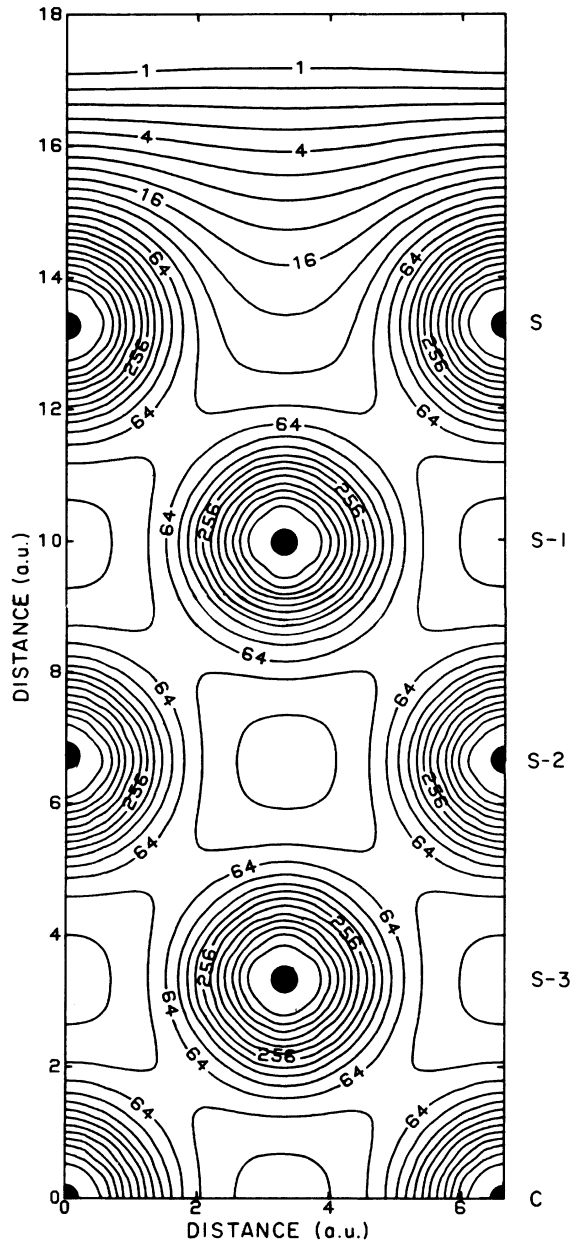


FIG. 6. Self-consistent charge-density map in units of 0.001 a.u. on the (110) plane. Each contour line differs by a factor of $\sqrt{2}$.

face and subsequent layers) and spin magnetic-moment values of 0.44 , 0.58 , 0.62 , 0.56 , and $0.54\mu_B$. The spin magnetic moments close to the center plane are in very good agreement with the experimental value³¹ of $0.56\mu_B$ and are slightly smaller than the theoretical value⁹ ($0.58\mu_B$) for bulk Ni. On the surface, the spin magnetic density, $0.44\mu_B$, is 20% smaller than that of the center plane; this reduction is consistent with field emission⁵ experiments. The max-

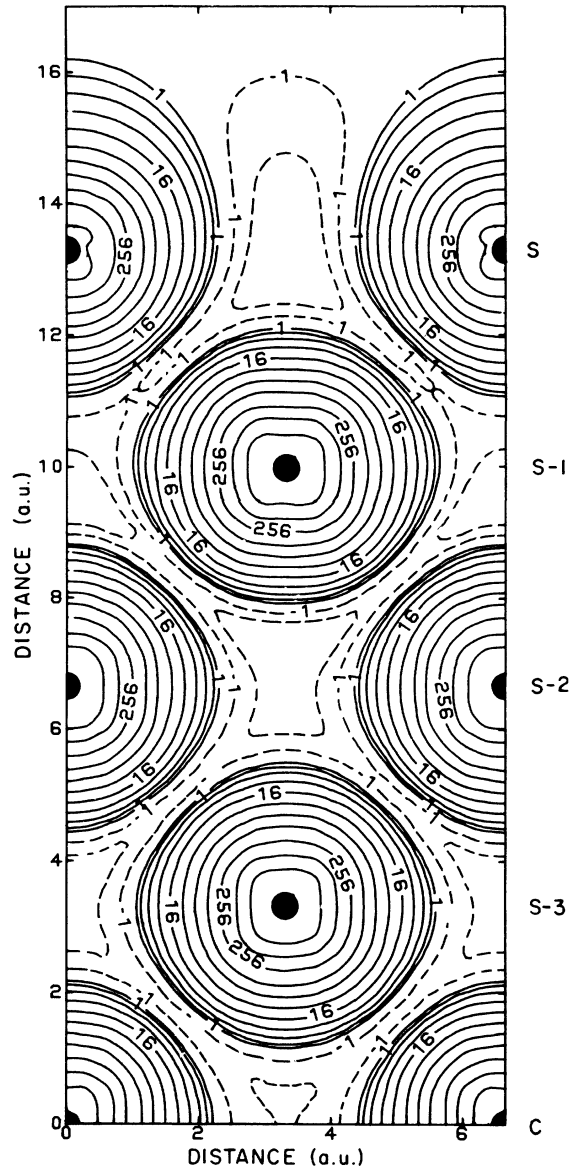


FIG. 7. Self-consistent spin-density map in units of 0.0001 a.u. on the (110) plane. Each contour line differs by a factor of 2. The dashed lines indicate negative spin density.

imum magnetic moment in the Friedel-type oscillation in the spin density which occurs two layers below the surface indicates the inapplicability of studying surface magnetism relevant to semi-infinite solids with ultrathin films (less than nine layers) either experimentally or theoretically.

Whereas ultrathin films were considered originally to be ideal systems for studying surfaces because of their large surface to volume ratio, it is now clear that a finite thickness may severely modify the SS responsible for the changes in ESP on the surface.

Experiments with ultrathin films deposited on a nonmagnetic substrate are further complicated by (i) the influence on the SS of the magnetic metal and the nonmagnetic substrate interface, (ii) possible additional localized interface states, and (iii) the reduction of the observed total ESP by photoemission from the nonmagnetic substrate. Hence, the magnetically "dead" layers reported earlier⁴ are not directly comparable with results of spin polarization on the free surface of a magnetic metal.

ACKNOWLEDGMENTS

We are grateful to D. E. Ellis, D. D. Koelling, S. Bader, and M. Brodsky for helpful discussions and M. Brodsky for support and encouragement. Work supported by the National Science Foundation (Grant No. DMR 77-23776) and under the NSF-MRL program through the Materials Research Center of Northwestern University (Grant No. DMR 76-80847), and the Department of Energy.

*Present address: Dept. of Phys. and Astron., Univ. of Maryland, College Park, Md. 20742.

- ¹G. Busch, M. Campagna, and H. C. Siegmann, *Phys. Rev. B* **4**, 746 (1971).
- ²W. Eib and S. F. Alvarado, *Phys. Rev. Lett.* **37**, 444 (1976).
- ³D. E. Eastman, F. J. Himpsel, and J. A. Knapp, *Phys. Rev. Lett.* **40**, 1514 (1978).
- ⁴G. Bergmann, *Phys. Rev. Lett.* **41**, 264 (1978); M. Sato and K. Hirakawa, *J. Phys. Soc. Jpn.* **39**, 1467 (1975).
- ⁵M. Landolt and M. Campagna, *Phys. Rev. Lett.* **38**, 663 (1977) and references therein.
- ⁶D. Paraskevopoulos, R. Meservey, and P. M. Tedrow, *Phys. Rev. B* **16**, 4907 (1977).
- ⁷S. Eichner, C. Rau, and R. Sizmann, *J. Magn. Magn. Mater.* **6**, 204 (1977).
- ⁸R. J. Smith, J. Anderson, J. Hermanson, and G. L. La-peyre, *Solid State Commun.* **21**, 459 (1977).
- ⁹C. S. Wang and J. Callaway, *Phys. Rev. B* **15**, 298 (1977); J. Callaway and C. S. Wang, *Phys. Rev. B* **14**, 2095 (1977).
- ¹⁰V. L. Moruzzi, A. R. Williams, and J. F. Janak, *Calculated Electronic Properties of Metals* (Pergamon, New York, 1978).
- ¹¹T. E. Feuchtwang and P. H. Cutler, *Surf. Sci.* **75**, 401 (1978).
- ¹²E. P. Wohlfarth, *Phys. Rev. Lett.* **38**, 425 (1977); *Phys. Lett. A* **36**, 131 (1971).
- ¹³N. V. Smith and M. M. Traum, *Phys. Rev. Lett.* **27**, 1388 (1971).
- ¹⁴D. G. Dempsey and L. Kleinman, *Phys. Rev. Lett.* **39**, 1297 (1977); D. G. Dempsey, W. R. Grise, and L. Kleinman, *Phys. Rev. B* **18**, 1270 (1978).
- ¹⁵D. G. Dempsey, W. R. Grise, and L. Kleinman, *Phys. Rev. B* **18**, 1550 (1978).
- ¹⁶See the review by U. Gradmann, *J. Magn. Magn. Mater.* **6**, 173 (1977).
- ¹⁷L. N. Liebermann, D. R. Fredkin, and H. B. Shore, *Phys. Rev. Lett.* **22**, 539 (1969); L. N. Liebermann, J. Clinton, D. M. Edwards, and J. Mathon, *Phys. Rev. Lett.* **25**, 232 (1970).
- ¹⁸P. Fulde, A. Luther, and R. E. Watson, *Phys. Rev. B* **8**, 440 (1973).
- ¹⁹K. Levin, A. Liebsch, and K. H. Bennemann, *Phys. Rev. B* **7**, 3066 (1973).
- ²⁰M. C. Desjonguères and F. Cyrot-Lackmann, *Solid State Commun.* **20**, 855 (1976).
- ²¹D. M. Edwards, in *Proceedings of the 4th EPS General Conference*, edited by M. M. Woolfson (Hilger, London, 1979), p. 150.
- ²²G. Bergmann, *Phys. Today* **32**, 25 (1979) contains his recent review of his experiments. Also see references therein and Ref. 4 above.
- ²³C. S. Wang and A. J. Freeman, *Phys. Rev. B* **19**, 793 (1979).
- ²⁴C. S. Wang and A. J. Freeman, *Phys. Rev. B* **10**, 4930 (1979).
- ²⁵U. von Barth and L. Hedin, *J. Phys. C* **5**, 1679 (1972).
- ²⁶W. Plummer and W. Eberhardt (unpublished).
- ²⁷E. Caruthers, L. Kleinman, and C. P. Alldredge, *Phys. Rev. B* **8**, 4570 (1973).
- ²⁸I. D. Moore and J. B. Pendry (unpublished).
- ²⁹J. B. Pendry and J. F. L. Hopkinson, *J. Phys. F* **8**, 1009 (1978).
- ³⁰C. S. Wang and J. Callaway, *Phys. Rev. B* **9**, 4897 (1974); D. Laurent, J. Callaway, and C. S. Wang, *Phys. Rev. B* **20**, 1134 (1979).
- ³¹H. Dannan, R. Herr, and A. J. P. Meyer, *J. Appl. Phys.* **39**, 669 (1968).